# Stratospheric water vapor and ozone response to different QBO disruption events in 2016 and 2020

Mohamadou Diallo[1], Felix Ploeger[2], Michaela Imelda Hegglin[3], Manfred Ern[2], Jens-Uwe Grooss[1], Sergey M. Khaykin[4], and Martin Riese[2]

[1]Institute of Energy and Climate Research, Stratosphere (IEK–7), Forschungszentrum Juelich, 52 425 Juelich, Germany.
[2]Forschungszentrum Juelich
[3]University of Reading
[4]CNRS-LATMOS

November 22, 2022

### Abstract

The Quasi-Biennial Oscillation (QBO) is a major mode of climate variability with periodically descending westerly and easterly winds in the tropical stratosphere, modulating transport and distributions of key greenhouse gases such as water vapor and ozone. In 2016 and 2020, anomalous QBO easterlies disrupted the QBO's 28–month period previously observed. Here, we quantify the impact of these QBO disruptions on lower stratospheric circulation, and water vapour and ozone using reanalyses and satellite observations, respectively. Both constituents decrease globally from early spring to late autumn during 2016, while they only weakly decrease during 2020. These dissimilarities result from differences in upwelling and cold-point tropopause temperatures caused by anomalous planetary and gravity wave forcing. Our results highlight the need for a better understanding of the causes of QBO disruptions, their interplay with other modes of climate variability, and their impacts on water vapor and ozone in the face of a changing climate.

# Stratospheric water vapor and ozone response to different QBO disruption events in 2016 and 2020

**Mohamadou Diallo[1], Felix Ploeger[1,2], Michaela I. Hegglin[3], Manfred Ern[1], Jens-Uwe Grooß[1], Sergey Khaykin[4] and Martin Riese[1,2]**

[1]Institute of Energy and Climate Research, Stratosphere (IEK–7), Forschungszentrum Jülich, 52 425 Jülich, Germany.
[2]Institute for Atmospheric and Environmental Research, University of Wuppertal, Wuppertal, Germany.
[3]Department of Meteorology, University of Reading, Reading, UK.
[4]Laboratoire Atmosphères, Milieux, Observations Spatiales, UMR CNRS 8190, IPSL, Sorbonne Univ./UVSQ, Guyancourt, France.

## Key Points:

- The QBO disruptions in both 2016 and 2020 decreased lower stratospheric water vapor and ozone.
- There are significant differences in the strength and depth of the impacts of the two QBO disruption events due to diffrences in tropical upwelling and cold point temperature.
- The differences in tropical upwelling and cold point temperature are caused by stronger planetary and gravity wave breaking in the lower stratosphere in 2016 than in 2020.

Corresponding author: Mohamadou Diallo, `m.diallo@fz-juelich.de`

## Abstract

The Quasi-Biennial Oscillation (QBO) is a major mode of climate variability with periodically descending westerly and easterly winds in the tropical stratosphere, modulating transport and distributions of key greenhouse gases such as water vapor and ozone. In 2016 and 2020, anomalous QBO easterlies disrupted the QBO's 28–month period previously observed. Here, we quantify the impact of these QBO disruptions on lower stratospheric circulation, and water vapour and ozone using reanalyses and satellite observations, respectively. Both constituents decrease globally from early spring to late autumn during 2016, while they only weakly decrease during 2020. These dissimilarities result from differences in upwelling and cold-point tropopause temperatures caused by anomalous planetary and gravity wave forcing. Our results highlight the need for a better understanding of the causes of QBO disruptions, their interplay with other modes of climate variability, and their impacts on water vapor and ozone in the face of a changing climate.



## Plain Language Summary

The Quasi-Biennial Oscillation (QBO) is one of the key atmospheric modes of climate variability as it modulates the stratospheric Brewer-Dobson circulation (BDC) and composition in the stratosphere and troposphere. The quasi-periodic pattern of alternating QBO easterlies and westerlies was subject to two disruptions during the 2015–2016 and 2019–2020 winters, therefore, leading to lower stratospheric anomalous circulation and composition. Besides similarities in many respects, our analysis shows differences in the strength and depth of the stratospheric circulation and upper troposphere/lower stratosphere (UTLS) composition response to the 2015–2016 and 2019–2020 QBO disruptions. These differences are mainly caused by differences in the the strength and depth of the forcing of the atmospheric circulation by planetary and gravity waves, which may be associated with the anomalous regional surface conditions such as the strong El Niño Southern Oscillation (ENSO) in 2015–2016, the strong Indian Ocean Dipole (IOD) as well as the particularly warmer stratosphere of the Southern Hemisphere midlatitudes linked to Australian wildfire smoke in 2019–2020. Our results suggest a need of better understanding the interplay between QBO phases, ENSO events and IOD events in future climate change as it may have a large impact on the UTLS composition and its changes.


## 1 Introduction

The upper troposphere and lower stratosphere (UTLS) is a key region of the Earth climate system because of its large sensitivity to radiative forcing of greenhouse gases, such as water vapor ($H_2O$) and ozone ($O_3$) (Gettelman et al., 2011; Dessler et al., 2013; Nowack et al., 2015). Any changes in the composition of these radiatively active trace gases in the UTLS region lead to large impact on surface climate (e.g., Forster & Shine, 2002, 1999; Solomon et al., 2010; Riese et al., 2012). Ozone is mainly produced in the middle stratosphere and is a good proxy of the tropical upwelling. In addition, ozone variability in the tropical lower stratosphere is affected by variability in tropical upwelling (Randel et al., 2007; Abalos et al., 2013). The ozone transport and lifetime in the UTLS region are both modulated by the seasonality in the stratospheric circulation and the natural modes of climate variability, including the Quasi-Biennial Oscillation (QBO) (Randel & Thompson, 2011; Diallo et al., 2018). Lower stratospheric water vapor and its multi-timescale variations ranging from day to decades are mainly controlled by changes in the tropical cold point tropopause temperatures and its modulations by the natural variability, including the QBO (Holton & Gettelman, 2001; Hu et al., 2016; Tao et al., 2019). Therefore, the amount of water vapor in the UTLS region is directly linked to the dehydration in the air parcels crossing through the coldest temperatures in the tropical tropopause layer(e.g., between 14 and 19 km; Fueglistaler et al., 2009).

Considered as a dominant mode of variability of the equatorial stratosphere, the QBO globally impacts the transport and distributions of stratospheric water vapor and ozone. Mostly driven by gravity waves and equatorially trapped waves, the QBO is a quasi-periodic oscillation between tropical westerly and easterly zonal wind shears (Baldwin et al., 2001; Ern et al., 2014). Both phases modulate the vertical and meridional components of the stratospheric circulation and affect temperature structure, therefore, impacting the water vapor and ozone composition and radiative feedback in the UTLS region (Niwano et al., 2003; Diallo et al., 2019).

The quasi-periodic QBO cycle of about 28–month period, which alternates between westerly and easterly zonal wind shears, was subject to two disruptions in the past five years. In January 2016 and 2020, the anomalous QBO westerlies in the tropical lower stratosphere were unexpectedly interrupted by anomalous QBO easterlies created by combination of planetary waves propagating from the middle latitudes and equatorial convective gravity waves (Osprey et al., 2016; Coy et al., 2017; Hitchcock et al., 2018; Kang et al., 2020; Kang & Chun, 2021). There is not yet a clear understanding of how these QBO disruptions are linked to anomalously warm or cold sea surface temperatures (Taguchi, 2010; Schirber, 2015; Dunkerton, 2016; Christiansen et al., 2016; Barton & McCormack, 2017), volcanic aerosols (Kroll et al., 2020; DallaSanta et al., 2021), wildfire smoke (Khaykin et al., 2020; Yu et al., 2021) and climate changes (Anstey et al., 2021a). However, recent study based on climate model simulations from phase six of the Coupled Model Intercomparison Project (CMIP6) predicts increased disruption frequencies to the quasi-regular QBO cycle in a changing climate (Osprey et al., 2016; Anstey et al., 2021a). Previous studies also suggest that the QBO amplitude in the tropical stratosphere is decreasing in the lower stratosphere due to the climate change–induced strengthening of tropical upwelling (Saravanan, 1990; Kawatani et al., 2011; Kawatani & Hamilton, 2013). Thus, in the context of a changing climate, the predictable QBO signal associated with the quasi-regular phase progression and amplitude as well as its potential impacts on UTLS composition faces an uncertain future. Therefore, it is of particular importance to quantify and better understand the different impact of the QBO disruptions on changes in UTLS water vapor and ozone, which have the potential to impact the global radiative forcing of climate (Forster & Shine, 1999; Butchart & Scaife, 2001; Solomon et al., 2010; Riese et al., 2012).

Here, we quantify the similarity and differences in the strength and depth between the 2015–2016 and 2019–2020 QBO disruption impacts on lower stratospheric water vapor and ozone from satellite observations. Also, we analyse the main drivers of the differences in anomalous circulation and UTLS composition changes. Section 2 describes the satellite observational data sets and the regression model used for the quantification. Section 3 describes the anomalous stratospheric circulation and UTLS composition changes following the 2016 and 2020 events. Section 4 discusses the results of a regression analysis to provide evidence for the impact of the QBO disruptions on stratospheric water vapor and ozone together with the main reasons of the anomalous circulation and composition differences between the 2015–2016 and 2019–2020 QBO disruption impacts related to planetary and gravity wave dissipation. Finally, we discuss our results in the context of the anomalous surface conditions, including the strong El Niño Southern Oscillation (ENSO) in 2015–2016, the strong Indian Ocean Dipole (IOD) as well as the particularly warmer stratosphere linked to Australian wildfire smoke in 2020.

## 2 Data and methodology

To quantify the QBO impact, we used the monthly mean ozone and water vapor mixing ratios from the Aura Microwave Limb Sounder (MLS) satellite observations covering the 2013–2020 period (Livesey et al., 2017). The version 4.4 MLS data set used here has a vertical resolution of 2.5–3 $km$ ranging from 8 to 35 $km$ and 60 °S/N with a high precision and lower systematic uncertainty (Santee et al., 2017). Previous findings show that MLS zonal monthly mean $H_2O$ mixing ratios show very good agreement with the multi-instrument mean (Hegglin et al., 2013, 2021).

In addition to the MLS data set, we also utilize the temperature ($T$) and zonal mean wind ($U$) from the ERA5 reanalysis of the European Centre for Medium-Range Weather Forecasts (ECMWF) (Hersbach et al., 2020). We have also calculated the residual vertical velocity ($\overline{w^*}$) using the Transformed Eulerian Mean (TEM; Andrews et al. (1987)) and decomposed the wave drag into planetary and gravity wave contributions to the circulation anomalies (Ern et al., 2014, 2021). For more details about the ERA5 TEM calculations and wave decomposition see Diallo et al. (2021).

We disentangle the QBO impact on these monthly mean stratospheric water vapor and ozone mixing ratios from the other sources of natural variability by using a hybrid multiple regression model (Eq. 1). This established regression method is appropriate to separate the relative influences of the considered modes of climate variability, including the QBO, on stratospheric water vapor and ozone. Additional details about the prediction model and its applications can be found in Diallo et al. (2018). Our regression model decomposes the given monthly zonal mean variable, $Var_i$, into a long-term linear trend, seasonal cycle, modes of climate variability and a residual ($\epsilon$). For a given variable $Var_i$ (herein $O_3$, $H_2O$, (T), $\overline{w^*}$, PWD and GWD), the prediction model yields

$$\begin{aligned} Var_i(t_{month}, y_{lat}, z_{alt}) \quad &= Trend(t_{month}, y_{lat}, z_{alt}) + SeasCyc(t_{month}, y_{lat}, z_{alt}) + \\ &\sum_{n=1}^{5} b_n(y_{lat}, z_{alt}) \cdot Proxy_n(t_{month} - \tau_n(y_{lat}, z_{alt})) + \\ &\epsilon(t_{month}, y_{lat}, z_{alt}), \end{aligned} \tag{1}$$

where $Proxy_n$ represents the different climate indexes used here. $Proxy_1$ is a normalized QBO index (QBOi) from CDAS/Reanalysis zonally averaged winds at $50\,hPa$ (Kalnay et al., 1996). $Proxy_2$ is the normalized Multivariate ENSO Index (MEI; Wolter & Timlin, 2011), $Proxy_3$ is the Indian Ocean Dipole (IOD, Saji et al., 1999), $Proxy_4$ is the Madden-Julian Oscillation (MJO, Son et al., 2017), and $Proxy_5$ is the AOD from satellite data (Thomason et al., 2018). $Trend(t_{month}, y_{lat}, z_{alt})$ are a linear trend. $SeasCyc(t_{month}, y_{lat}, z_{alt})$ is the annual cycle. The coefficients are the amplitude $b_n$ and the lag $\tau_n(y_{lat}, z_{alt})$ associated with the QBO, ENSO, IOD, MJO and AOD respectively. The solar forcing is neglected because our data set is relatively short and covers less than one 11-year solar cycle. Finally, we estimate the uncertainty in the statistical prediction using a Student's $t$ test technique (von Storch & Zwiers, 1999; Friston et al., 2007).

## 3 Characterisation of the 2016 and 2020 anomalous circulations

In January 2016 and 2020 unexpected tropical QBO easterlies (negative QBOi) developed in the center of the tropical QBO westerlies, thereby breaking the quasi-regular QBO cycle of alternating easterly and westerly phases (Osprey et al., 2016; Newman et al., 2016; Anstey et al., 2021b). Both QBO disruptions have been associated with a combination of extratropical Rossby waves, equatorial planetary waves (Kelvin, Rossby, mixed Rossby–gravity, and inertia–gravity), and small-scale convective gravity waves, propagating into the deep tropics and depositing their negative momentum forcing (Osprey et al., 2016; Newman et al., 2016; Kang et al., 2020; Kang & Chun, 2021). Although similar in many respects, including the causes of the sudden development of tropical QBO easterlies in the center of tropical QBO westerlies, the two disruptions also exhibit differences, in particular how the wave forcing triggered the events as in the structure (strength and depth) of the impacts and the level at which it started. While the 2015–2016 QBO disruption is primarily triggered by mid-latitude Rossby waves propagating from the northern hemisphere into the deep tropics, the 2019–2020 QBO disruption is initially triggered by the equatorial planetary and small-scale convective gravity waves propagating into the UTLS (Kang et al., 2020; Kang & Chun, 2021).

The similarities as well as the differences between the two disruption events are also visible in the inter-annual variability of the tropical lower stratospheric zonal mean wind (a), $H_2O$ (b) and $O_3$ (c) anomalies as a percentage change relative to the monthly mean mixing ratio during the 2013–2020 period (Fig. 1a–c). Both QBO disruptions are expected to impact the tropical upwelling, via wave–mean-flow interaction (Holton, 1979; Dunkerton, 1980; Grimshaw, 1984) and control of the tropical cold point temperatures (Kim & Son, 2012; Kim & Alexander, 2015). This impact of the 2015–2016 and 2019–2020 QBO disruptions on the transport and distribution of lower stratospheric $H_2O$ (b) and $O_3$ (c) is the most effective when the signal reaches the tropopause level e.g. from June to August (Fig. 1a, d) (Tweedy et al., 2017; Diallo et al., 2018). The zonal mean wind shows that the QBO disruption is stronger and deeper in 2015–2016 than in 2019–2020 regarding the westerly jet at $30\,hPa$ (Fig. 1a and Fig. S1a–b in the supplement). The 2019–2020 QBO disruption shows a clear cut of the westerlies in two parts while the 2015–2016 QBO disruption shifts the westerlies upward (Fig. 1a). As soon as the downward propagation of tropical QBO easterlies reaches the tropical tropopause ($\sim$16 $km$) around June–August 2016, the $H_2O$ mixing ratios start to decrease i.e. turning from positive to negative anomalies. As reported by (Diallo et al., 2018), the alignment of the strong El Niño event with westerly QBO in early boreal winter of 2015–2016 substantially increased $H_2O$ and decreased $O_3$ in the tropical lower stratosphere (Fig. 1b, c). Then, the sudden occurrence of the QBO disruption led to a lower stratospheric $H_2O$ and $O_3$ decrease from late spring to early following winter.

Conversely, during the 2019–2020 QBO disruption, Figure 1b, c show clear differences in the tropical lower stratospheric trace gas anomalies, particularly in the strength and depth of $H_2O$ and $O_3$ anomalies consistent with the zonal wind changes (Fig. 1a). The tropical lower stratospheric $O_3$ anomalies are purely responding to the enhanced tropical upwelling caused by a combination of a strong El Niño event, negative IOD event and the QBO disruption in 2015–2016, and caused by a combination of a weak La Niña, strong positive IOD event and the QBO disruption in 2019–2020 (e.g., easterly winds at 100–40 $hPa$). However, the tropical lower stratospheric $H_2O$ variability (tape recorder) is more challenging to interpret because of its regulation by the variability in the tropical cold point temperatures (Holton & Gettelman, 2001; Hu et al., 2016). In 2020, the QBO disruption–induced tropical lower stratospheric $H_2O$ anomalies are weaker than in 2016, consistent with the zonal mean wind anomalies (Fig. 1a, Fig. S1a–d and Fig. S2a–d in the supplement). Particularly, the 2020 tape recorder shows large positive $H_2O$ anomalies even after the disruption that are of opposite sign to the 2016 $H_2O$ anomalies (Fig. 1b, c). This complexity in $H_2O$ inter-annual variability lies in its dependency on the interplay of different modes of natural variability, including the QBO phases (Diallo et al., 2018; Tian et al., 2019; Liess & Geller, 2012), seasons (early or late in the winter) and location (western, central or eastern Pacific, where the ENSO and IOD maximum occurs (Garfinkel et al., 2013; Smith et al., 2021)). Therefore, to elucidate the effect of both QBO disruptions on the lower stratospheric $H_2O$ and $O_3$ anomalies, we performed regression analysis both without and with explicitly including QBO signals to isolate the QBO impact on these trace gases. The difference between the residual ($\epsilon$ in Eq. 1) with and without explicit inclusion of the QBO signals gives the QBO–induced impact on stratospheric $H_2O$ and $O_3$ anomalies. This approach of differencing the residuals is similar to direct calculations, projecting the regression fits onto the QBO basis functions, i.e., the QBO predictor timeseries (see supplement Figs. 2 and 4 in (Diallo et al., 2017)). In addition, this differencing approach avoids the need to reconstruct the time series after the regression analysis.

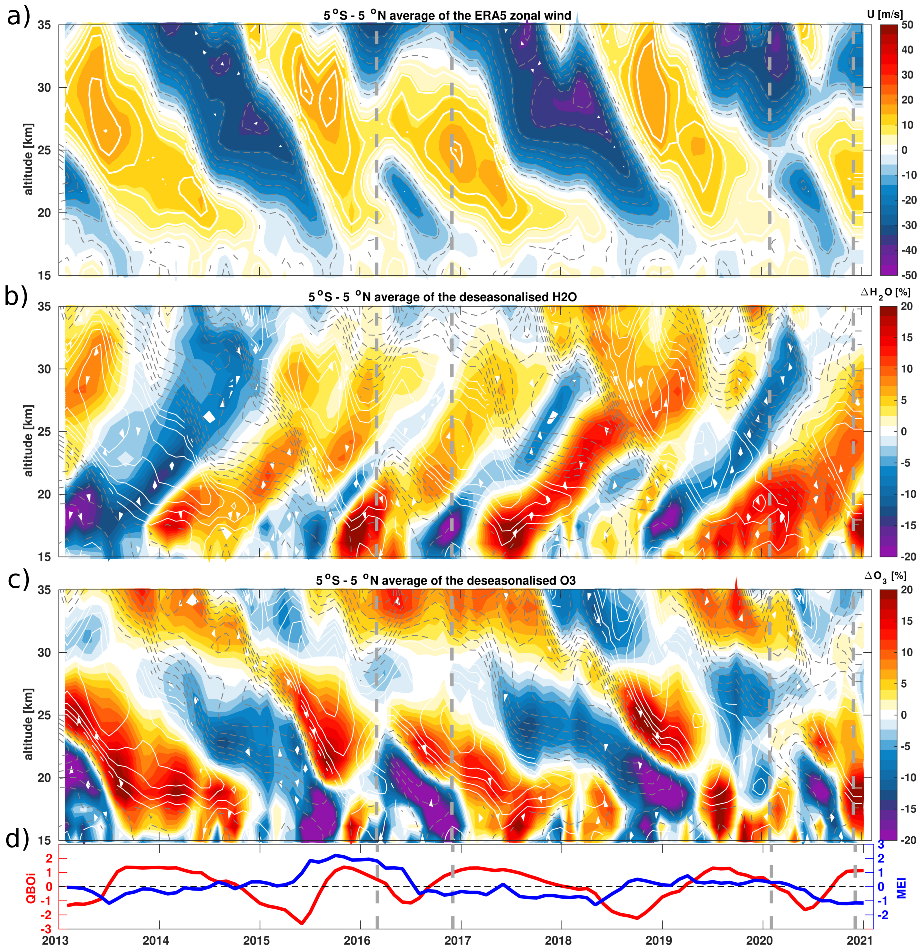


**Figure 1.** Tropical zonal mean zonal wind (U) from ERA5 **(a)** and deseasonalized tropical stratospheric $H_2O$ and $O_3$ time series from MLS satellite observations for the 2013–2020 period in percent change from long-term monthly means as a function of time and altitude. **(a)** Zonal mean wind U. **(b)** Deseasonalized monthly mean $H_2O$ anomalies. **(c)** Deseasonalized monthly mean $O_3$ anomalies. Vertical grey dashed lines indicate the QBO disruption onset and offset years. The lowermost panel **(d)** shows the QBO index at $50\,hPa$ in red and the MEI index in blue. Monthly averaged zonal mean zonal wind component, $u$ ($\mathrm{m\,s^{-1}}$), from ERA5, is overlaid as solid white (westerly) and dashed gray (easterly) lines.

# 4 Attribution to drivers using a statistical prediction model

## 4.1 Impact of QBO disruptions on UTLS composition

Figures 2a, b show time series of the QBO–induced inter-annual variability in tropical lower stratospheric $H_2O$ and $O_3$ anomalies estimated from the difference between the residual ($\epsilon$ in Eq. 1) without and with explicit inclusion of the QBO proxy for the 2013–2020 period. A footprint of both QBO disruptions is clearly visible in lower stratospheric $H_2O$ and $O_3$ anomalies with a shift from positive anomalies related to the westerly winds (positive QBOi) to negative anomalies related to the easterly winds (negative QBOi). The QBO disruption–induced $O_3$ anomalies are sudden and clearly follow the monthly mean zonal mean wind changes. The QBO disruption–induced $H_2O$ anomalies are roughly in phase with the zonal wind anomalies with a delay of about 3–6 months

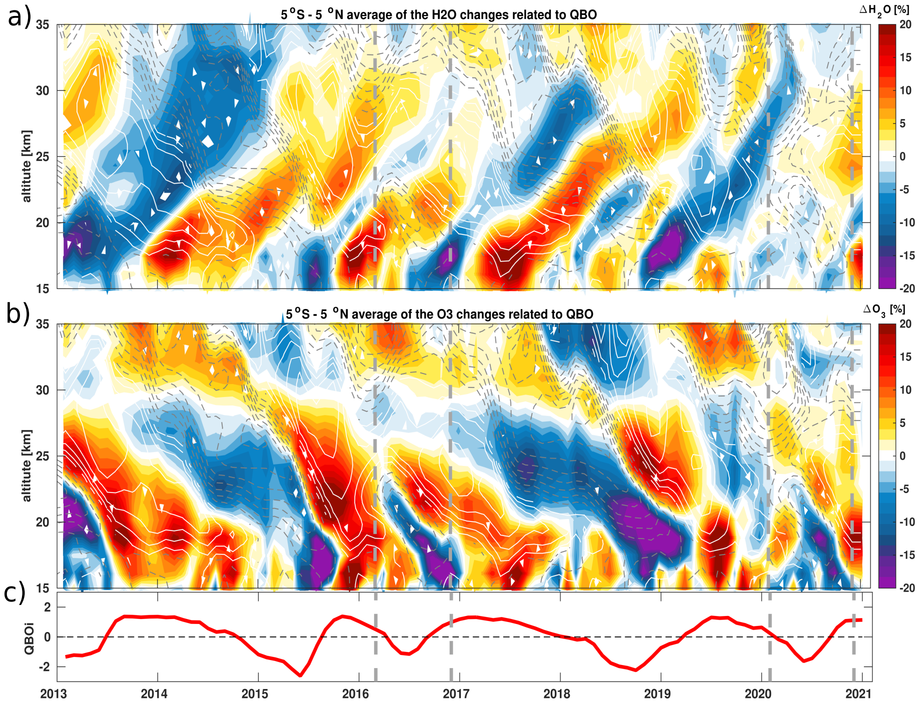


**Figure 2.** QBO impact on the stratospheric $H_2O$ **(a)** and $O_3$ **(b)** anomalies from the MLS satellite observations for the 2013–2020 period in percent change relative to monthly mean mixing ratios as a function of time and altitude. Shown QBO impact on the stratospheric trace gases is derived from the multiple regression fit as the difference between the residual ($\epsilon$ in Eq. 1) without and with explicit inclusion of the QBO signal. The lower panel below indicates the QBO index at $50\,hPa$ in red. Vertical grey dashed lines indicate the QBO disruption onset and offset years.

because of its tropospheric origin and its tropical cold point temperature anomaly dependency.

Beside the good agreement in the patterns of trace gas changes, there are clear differences in the strength and depth of the lower stratospheric $H_2O$ and $O_3$ response to the QBO disruptions between the 2016 and the 2020 events. These differences in the impact of the QBO disruption are consistent with the observed lower stratospheric $H_2O$ and $O_3$ anomalies (Fig. 1 and Fig. S2a–c). During 2016, the QBO shift from westerlies to easterlies at $40\,hPa$ in the tropical lower stratosphere induces substantial negative $H_2O$ and $O_3$ anomalies as large as $15\,\%$–$20\,\%$ between 16 and $20\,km$ from the early boreal spring to the next boreal winter. This decrease in $H_2O$ and $O_3$ mixing ratios is consistent with upward transport of young and dehydrated air poor in $H_2O$ and $O_3$ into the lower stratosphere (Fig. 2). As expected, the sudden occurrence of the QBO disruption causes anomalously cold point temperatures and stronger tropical upwelling, consistent with the strong decrease in $H_2O$ and $O_3$ mixing ratios.

However, besides the similarities in the structural changes, the QBO disruption induced–negative $H_2O$ and $O_3$ anomalies are smaller and shallower in 2020 than in 2016. The differences in the magnitude of negative $O_3$ anomalies suggest a weaker tropical upwelling anomalies of the stratospheric circulation in 2020 than in 2016, consistent with the differences in the strength and depth of the wave forcing anomalies discussed in Sect. 4.2.

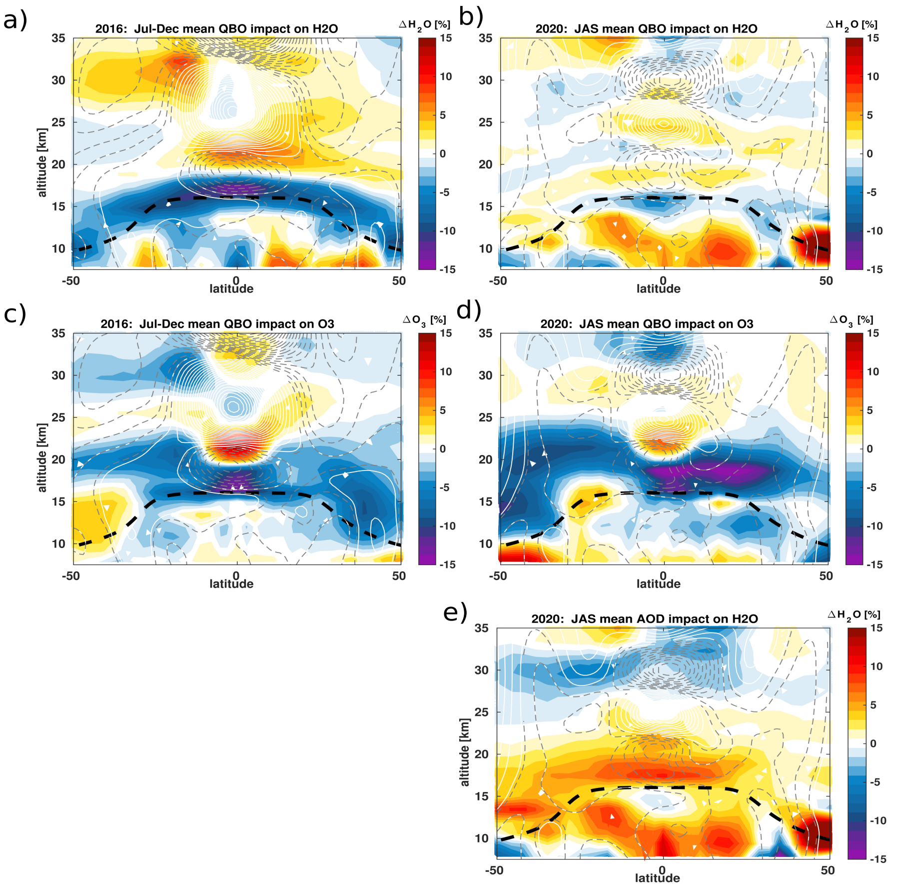


**Figure 3.** Zonal mean impact of the QBO disruption on the lower stratospheric $H_2O$ **(a, b)** and $O_3$ **(c, d)** anomalies from MLS satellite observations averaged from July to December for 2016 **(a, c)** and from July to September for 2020 **(b, d)** period. In addition, the impact of the 2020 Australian wildfires is shown **(e)**. All panels show the percentage change relative to monthly mean mixing ratios as a function of latitude and altitude. The impact of the QBO disruptions and the Australian wildfire on the stratospheric trace gases is derived from the multiple regression fit as the difference between the residual ($\epsilon$ in Eq. 1) without and with explicit inclusion of the QBO signal. The black dashed horizontal line indicates the tropopause from ERA5. Monthly mean zonal mean wind component, $u$ ($\mathrm{m\,s^{-1}}$), from ERA5 is overlaid as solid white (westerly) and dashed gray (easterly) lines.

The differences in the strength of $H_2O$ anomalies suggest that the impact of QBO disruptions on tropical cold point temperatures is substantially different between the year 2016 and year 2020. In addition, we note that the early QBO westerly followed by the shift to QBO easterly is not the main cause of the large increase in the 2020 lower stratospheric $H_2O$ anomalies. In the following, we assess the potential impact of the unusually strong Australian wildfire smoke on the lower stratospheric $H_2O$ anomalies in 2020 (Khaykin et al., 2020; Yu et al., 2021).

Figures 3a–b show the zonal mean impact of the QBO disruptions on lower stratospheric $H_2O$ and $O_3$ anomalies. Figure 3e shows the impact of 2020 Australian wildfire AOD on lower stratospheric $H_2O$ and $O_3$ anomalies. The lower stratospheric $H_2O$ anomalies are averaged from July to December for 2016 and from July to September for 2020 respectively. We chose different averaging periods for 2016 and 2020 because of the differences in the strength and depth of the QBO disruption–induced $H_2O$ and $O_3$ anomalies. These chosen periods highlight better the similarities in patterns and maximum ocurrence of the QBO impact on both trace gas anomalies as well as the differences in the strength and depths of $H_2O$ and $O_3$ responses.

In 2016, the shift to QBO easterly phase in the tropics significantly dehydrates the global lower stratosphere by about 10 to 15 % below 20 $km$ (Fig. 3a and Fig. S2a) (Diallo et al., 2018; Tweedy et al., 2017). This decrease in $H_2O$ mixing ratios is due to the enhanced tropical upwelling and related decrease of cold point temperature as discussed later in Sect. 4.2 (Jensen et al., 1996; Hartmann et al., 2001; Geller et al., 2002; Schoeberl & Dessler, 2011). Because of the asymmetry of the mean meridional mass circulation, which is driven by planetary wave activity (e.g. Holton & Gettelman, 2001) and eddy mixing (e.g. Haynes & Shuckburgh, 2000), the rising dehydrated air from the tropics moves toward middle and high latitudes of both hemispheres. The positive $H_2O$ anomalies above 20 $km$ are related to the effect of the preceding QBO westerly phase on TTL temperatures and the upward propagating tape-recorder signal. The changes in $H_2O$ anomalies are consistent with the observed tropical negative $O_3$ anomalies below 20 $km$ induced by the QBO easterly phase and indicate an enhanced tropical upwelling in the lower stratosphere (Fig. 3c and Fig. S2c in the supplement). Above 20 $km$, the positive tropical $O_3$ anomalies are associated with the QBO westerly phase between ((Fig. 3c and Fig. S2c in the supplement). Also note the large variability in extratropical $O_3$ anomalies related to the QBO influence on the extratropical circulation (Damadeo et al., 2014), stratospheric major warmings, and chemical processes (WMO, 2018).

In 2020, the patterns of QBO disruption–induced changes in tropical lower stratospheric $H_2O$ and $O_3$ anomalies exhibit similarities with the 2015–2016 QBO disruption effect. Both trace gases show negative anomalies in the tropics, corroborating the enhanced upwelling induced by the shift to QBO easterly phase in the tropics (Fig. 3b and Fig. S2b in the supplement). However, there are also large differences in the lower stratospheric trace gas response to the shift from the tropical QBO westerly phase to the tropical QBO easterly phase, particularly in $H_2O$ anomalies. Conversely to the globally dehydrated lower stratosphere in 2016, the sudden development of tropical QBO easterly in 2020 led to a smaller decrease in lower stratospheric $H_2O$ mixing ratios, therefore, to smaller lower stratospheric $H_2O$ anomalies (Fig. 3b and Fig. S2b in the supplement). In addition to the good agreement in the zonal mean structure of $O_3$ anomalies between both QBO disruptions, the changes in zonal mean $O_3$ mixing ratios induced by the 2019–2020 QBO disruption are also weaker in the tropics than for the 2015–2016 QBO disruption. The differences between the 2016 and 2020 $H_2O$ and $O_3$ anomalies clearly suggest substantial differences in the anomalous circulation and the tropical cold point temperatures. The weak negative tropical $O_3$ anomalies suggest that the tropical upwelling of the stratospheric circulation is slower and weaker in 2020 than in 2016. Simultaneously, the positive tropical $H_2O$ anomalies in 2020 indicate a warmer tropical cold point temperature. The main dynamical causes of these differences are investigated in the following section.

### 4.2 Mechanisms behind the strength and depth differences

To further investigate and understand the key drivers of the anomalous circulation differences between the 2015–2016 and 2019–2020 QBO disruptions, we analyse the differences in the residual vertical velocity ($\overline{w^*}$) and temperature anomalies. Figure 4a–c show tropical time series of the residual circulation vertical velocity and temperature anomalies together with the QBO disruption impacts on temperature anomalies during the 2015–2016 and 2019–2020 periods, respectively. Latitude-altitude sections of the residual circulation vertical velocity and temperatures together with the QBO disruption impacts on temperature anomalies during the 2015–2016 and 2019–2020 periods are shown in the supplement Fig. S3. Clearly, there are substantial differences in the tropical upwelling of the stratospheric circulation and temperatures for the two disruption events. In 2016, the tropical upwelling strongly increases up to about 20 $km$ when the QBO easterly phase reaches the tropopause (Fig. 4a). This enhancement of tropical upwelling during July-August-September (JAS) 2016 is also visible in the JAS zonal mean cross section of the mean residual vertical velocity and temperature anomalies (Fig S3a, b), together with the QBO disruption impacts on temperature anomalies (Fig. S3c in the supplement). However, the increase of the tropical upwelling is weaker and shallower in 2020 than in 2016 (Fig. 4a and Fig. S3a in the supplement). The differences in the anomalous tropical upwelling are also consistent with the differences in the QBO disruption–induced temperature anomalies (Fig. 4a, b and Fig. S3c–f in the supplement). In 2016, the tropical cold point temperature anomalies (at altitudes of about 17–18 $km$) are substantially negative. This decrease in tropical temperatures is consistent with the strong tropical upwelling, which, in turn led to large negative tropical lower stratosphere $H_2O$ and $O_3$ anomalies (Fig. 4 and Fig. S3a, c, e in the supplement). Conversely, the tropical cold point temperature anomalies are warmer and barely exceeding -0.1 $K$ in 2020, consistent with the weak tropical residual vertical velocity anomalies (Fig. 4 and Fig. S3b, d, f in the supplement) and not long lasting tropical $O_3$ anomalies i.e. about 3 months (Fig. 3 and Fig. S3b, d, f in the supplement). These warmer tropical cold point temperatures corroborate the slower tropical upwelling and the weaker tropical lower stratospheric $H_2O$ and $O_3$ anomalies in 2020. Interestingly, the differences in the tropical cold point temperature anomalies between 2016 and 2020 are more pronounced as shown in Figure S3c, d in the supplement than the differences in the QBO disruption–induced tropical cold point temperature anomalies (Figure S3e, f in the supplement). This anomalously warmer stratosphere, including warmer cold point temperature, in 2020 is consistent with recent findings about the impact of Australian wildfire smoke (Khaykin et al., 2020; Yu et al., 2021). Indeed using our regression analyses, we can show that the Australian wildfire largely moistened the lower stratosphere in 2020 by inducing anomalously warmer stratosphere, therefore, hidding the impact of 2019–2020 QBO disruption on $H_2O$ anomalies (Fig. 3e). The removal of Australian wildfire impact allows a better highlight of the weak and similar effect of the 2019–2020 QBO disruption on lower stratospheric $H_2O$ anomalies compared to 2015–2016 QBO disruption–induced effect. These differences are also reflected in the stratospheric circulation forcing, and we finally investigate the related wave drag changes in the following.

To investigate the main causes of the stratospheric circulation differences between the 2015–2016 and 2019–2020 QBO disruptions, we calculate the planetary and gravity wave drag. We analyse the differences in terms of wave activities potentially induced by specific sea surface conditions such as the unusually warm 2015–2016 El Niño and the 2019 strong positive Indian Dipole Ocean, which impact tropical convective activities (Jia et al., 2014). In addition, we also pay attention to volcanic eruptions and Australian wildfire smoke in 2020, which can impact lower stratospheric temperatures, and therefore, lower stratospheric $H_2O$ and $O_3$ anomalies. For additional details about the wave decomposition please see Diallo et al. (2021) and Ern et al. (2014).

The stratospheric circulation as well as its interannual variability are driven by the planetary and gravity wave breaking in different stratospheric regions (Haynes et al., 1991; Rosenlof & Holton, 1993; Newman & Nash, 2000; Plumb, 2002; Shepherd, 2007). Therefore, any changes in wave drag will lead to circulation and composition changes. Figure 5a–c show time series of deseasonalized monthly mean tropical net wave forcing (PWD + GWD - du/dt), planetary wave drag (PWD) and gravity wave drag from the ERA5 reanalysis for the 2013–2020 period as a function of time and altitude. Note that the net wave forcing is equal to the contribution of Coriolis force plus meridional advection plus vertical advection to the momentum balance (Ern et al., 2021). Clearly, the net forcing anomalies as well as the planetary and gravity wave drag anomalies exhibit differences in strength and depth in the lower stratosphere between the 2015–2016 and 2019–2020

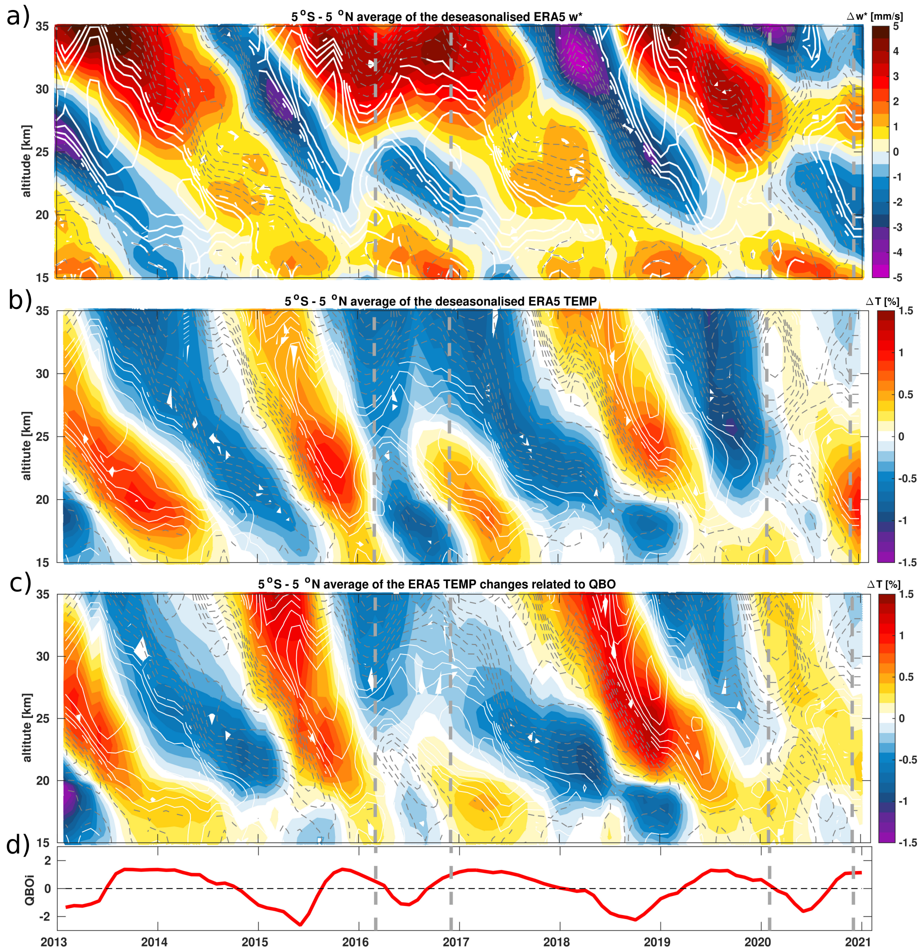


**Figure 4.** Deseasonalized tropical mean residual vertical velocity ($\overline{w^*}$) **(a)** and temperature anomalies **(b)** time series from ERA5 for the 2013–2020 period together with the impact of QBO disruptions on the tropical mean temperature anomalies **(c)** derived from the multiple regression fit as a function of latitude and altitude. **(a)** Deseasonalized monthly mean tropical upwelling. **(b)** Deseasonalized monthly mean tropical temperature. **(c)** QBO disruption impact on monthly mean tropical temperature anomalies. Vertical grey dashed lines indicate the QBO disruption onset and offset years. The lowermost panel shows the QBO index at 50 $hPa$ in red. Monthly averaged zonal mean zonal wind component, $u$ ($\mathrm{m\,s^{-1}}$), from ERA5, is overlaid as solid white (westerly) and dashed gray (easterly) lines.

QBO disruptions (Fig 5a–c). These differences in wave forcings are even clearer in the January-to-June averaged zonal mean net forcing, planetary and gravity wave drag, i.e. during six months (January–to–June) of the evolving QBO disruptions (Fig. S4 a–f in the supplement). During the 2015–2016 QBO disruption, the net wave forcing is stronger and broader in the lower stratosphere than during the 2019–2020 QBO disruption. Particularly, the wave breaking near the equatorward flanks of the subtropical jet known as BDC forcings region is narrower in 2020 than 2016 (Fig. S4 a, b in the supplement). These differences in net forcing are the main cause of a weaker stratospheric circulation impact in 2020 than in 2016, therefore, explaining the observed differences in lower stratospheric $H_2O$ and $O_3$ anomalies.

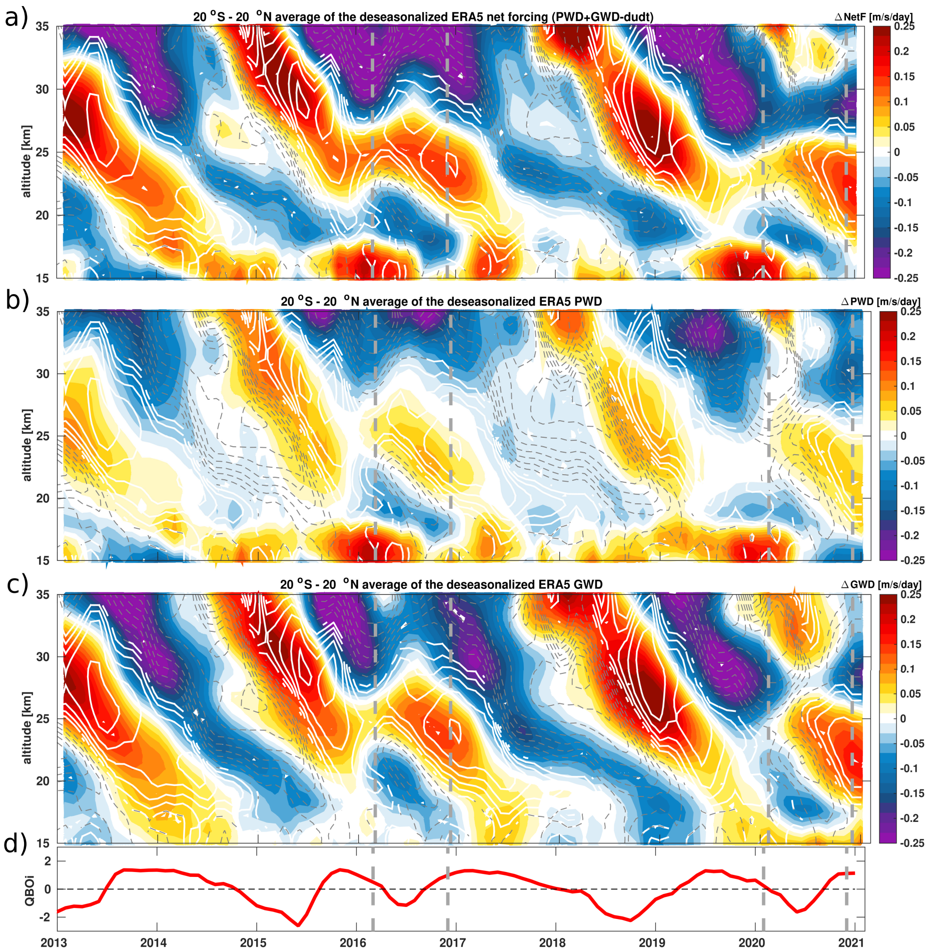


**Figure 5.** Deseasonalized monthly mean tropical net wave forcings (NetF) **(a)**, planetary wave (PWD) **(b)** drag and gravity wave (GWD) **(c)** drag time series from ERA5 for the 2013–2020 period as a function of time and altitude. **(a)** Deseasonalized monthly mean tropical net wave forcing. **(b)** Deseasonalized monthly mean tropical PWD drag. **(c)** Deseasonalized monthly mean tropical PWD drag. Vertical grey dashed lines indicate the QBO disruption onset and offset years. The lowermost panel shows the QBO index at $50\,hPa$ in red. Monthly averaged zonal mean zonal wind component, $u$ ($\mathrm{m\,s^{-1}}$), from ERA5, is overlaid as solid white (westerly) and dashed gray (easterly) lines.

In addition, we show the contribution of planetary (Fig 5b, and Fig. S4c, d) and gravity (Fig 5c and Fig. S4e, f) wave drag to better understand the role of each forcing during both QBO disruptions. Beside the good agreement in the pattern of planetary and gravity wave breaking, our analyses also show differences between the 2015–2016 and 2019–2020 disruptions in wave drag. The planetary and gravity wave drag indicates stronger anomalies in wave dissipation in the lower stratosphere during the 2015–2016 QBO disruption than during the 2019–2020 QBO disruption (Fig. 5b, c and Fig. S4c–f in the supplement). The anomalies in planetary wave dissipation associated with the 2015–2016 QBO disruption are stronger and extends from the tropics toward the subtropical jet, while for the 2019–2020 disruption, these anomalies are weaker and confined to the tropics. These differences in the strength and depth of the anomalies are even larger in the gravity wave drag. During the 2015–2016 QBO disruption, gravity waves break in the entire lower stratosphere with a maximum occurring near the upper flank of the subtropical jet, a key region for strengthening the shallow branch of the stratospheric circulation (Shepherd & McLandress, 2011; Diallo et al., 2019, 2021) (Fig. 5b and Fig. S4 c, d in the supplement). The differences in the strength and depth of planetary and gravity wave breaking are clearly the main cause of observed differences in the tropical upwelling and cold point temperature between the 2015–2016 and 2019–2020 QBO disruptions. The main cause is a combination of planetary wave dissipation in the tropics and particularly strong gravity wave breaking near the equatorward flanks of the subtropical jet during the 2015–2016 QBO disruption, consistent with previous studies (Kang et al., 2020; Kang & Chun, 2021; Osprey et al., 2016). Note that during the 2015–2016 and 2019–2020 QBO disruptions, the surface conditions were different in terms of natural variability–induced convective activity.

To trace back the potential source of convectively generated wave activities to regional differences, we finally analysed the monthly mean Outgoing Longwave Radiation (OLR) (Fig. S5 a, b in the supplement). Clearly, there are regional differences in the occurrence of strong convective events between the 2015–2016 and 2019–2020 QBO disruptions. During the 2015–2016 QBO disruption, the tropical mean OLR anomalies reveal two active convective regions, namely the East Indian Ocean associated with the negative IOD in 2016, and the Central Pacific Ocean associated with the 2015–2016 El Niño. However, during the 2019–2020 QBO disruption, the tropical mean OLR anomalies show only one strong active convective region that is the West Indian Ocean and East Africa associated with the strong 2019 IOD. Both QBO disruption effects related to OLR variations exhibit strong convective activity in the Indian Ocean, therefore suggesting the importance role of this region may play. This additional information is valuable for better understanding and relating the origin of the QBO disruption and its strength based on regional forcings. This regional forcing and interplay of different modes of climate variability will be presented in further studies.

## 5 Summary and conclusions

Based on an established multiple regression method applied to Aura MLS observations, we found that both the 2015–2016 and 2019–2020 QBO disruptions induced similar structural changes in the lower stratospheric $H_2O$ and $O_3$. Both QBO disruptions induced negative anomalies in $H_2O$ and $O_3$, few months after the sudden shift from the QBO westerly to QBO easterly winds reaches the tropical tropopause. During the boreal winter of 2015–2016 (September 2015–March 2016), the alignment of the strong El Niño with the QBO westerly strongly moistened the lower stratosphere (positive anomalies of more than 20 %). Analogously, the alignment of the weak El Niño with the strong QBO westerly and the impact of Australian wildfire smoke strongly moistened the lower stratosphere (positive anomalies of more than 20 %) during the boreal winter of 2019–2020 (September 2019–Jun 2020). The sudden shift from the QBO westerly to QBO easterly wind shear reversed the lower stratospheric moistening between the tropopause and $20\,km$, therefore leading to negative $H_2O$ and $O_3$ anomalies by the end of summers 2016 and 2020. These decreases in $H_2O$ and $O_3$ mixing ratios are due to a strengthening of the tropical upwelling and cooling tropical cold point temperatures, consistent with the residual vertical velocity and temperature anomalies.

However, major differences occur in the strength and depth of the QBO disruption–induced negative $H_2O$ and $O_3$ anomalies between 2016 and 2020. We found that the impact of the 2019–2020 QBO disruption on lower stratospheric $H_2O$ and $O_3$ anomalies is weaker and shallower than the 2015–2016 QBO disruption impact. These differences in the strength and depth between the 2015–2016 QBO and 2019–2020 QBO disruption impacts are due to discrepancies in the tropical upwelling and tropical cold point temperature anomalies induced by the differences in wave forcing. The analyses of wave forcings show that net wave forcing in the lower stratosphere, particularly the planetary and gravity wave drag, were stronger during the 2016–2016 QBO disruption than during the 2019–2020 QBO disruption. The differences in planetary wave breaking in the tropical lower stratosphere and the gravity wave breaking in the equatorward upper flank of the subtropical jet are the main reasons of the stratospheric circulation and cold point temperature differences between the 2015–2016 and 2019–2020 QBO disruptions and their impact on lower stratospheric $H_2O$ and $O_3$ anomalies.

Finally, our results suggest that the interplay of QBO phases with a combination of ENSO and IOD events, and in particular also wild fires and volcanic eruptions, will be crucial for the control of the lower stratospheric $H_2O$ and $O_3$ budget in a changing future climate. Especially, when increasing future warming will lead to trends in ENSO (Timmermann et al., 1999; Cai et al., 2014) and IOD (Ihara et al., 2008) as projected by climate models, and a related potential increase in wildfire frequency combined with a decreasing lower stratospheric QBO amplitude (Kawatani & Hamilton, 2013) are expected in future climate projections. The interplay will change with strong El Niño/negative IOD and La Niña/strong positive IOD likely controlling the lower stratospheric trace gas distributions and variability more strongly in a future changing climate. Clearly, both ENSO and IOD impact on the tropopause height and tropical cold point temperature. Further analysis is needed using climate model sensitivity simulations to pinpoint the impact of these future changes in lower stratospheric trace gases and the related radiative feedback.

**Acknowledgments**

Mohamadou Diallo research position is funded by the Deutsche Forschungsgemeinschaft (DFG) individual research grant number DI2618/1-1 and Institute of Energy and Climate Research, Stratosphere (IEK-7), Forschungszentrum in Jülich during which this work had been carried out. FP is funded by the Helmholtz Association under grant number VH-NG-1128 (Helmholtz Young Investigators Group A-SPECi). Manfred Ern was supported by the German Federal Ministry of Education and Research (Bundesministerium für Bildung und Forschung, BMBF) project QUBICC, grant number 01LG1905C, as part of the Role of the Middle Atmosphere in Climate II (ROMIC-II) programme of BMBF. We gratefully acknowledge the Earth System Modelling Project (ESM) for funding this work by providing computing time on the ESM partition of the supercomputer JUWELS at the Jülich Supercomputing Centre (JSC). Moreover, we particularly thank the European Centre for Medium-Range Weather Forecasts for providing the ERA5 and ERA-Interim reanalysis data.

## Data Availability Statement

MLS water vapor and ozone data were obtained from the Goddard Earth Sciences Data and Information Services Center at es Center at doi.10.5067/Aura/MLS/DATA2508 and doi.10.5067/Aura/MLS/DATA2516, respectively. The aerosol optical depth data is available through Khaykin et al. 2020. The ERA5 reanalysis are available at

https://apps.ecmwf.int/data-catalogues/era5/?class=ea, last access: 2nd February 2022, through Hersbach et al., 2020.

## References

Abalos, M., Ploeger, F., Konopka, P., Randel, W. J., & Serrano, E. (2013). Ozone seasonality above the tropical tropopause: reconciling the eulerian and lagrangian perspectives of transport processes. *Atmospheric Chemistry and Physics*, *13*(21), 10787–10794. doi: 10.5194/acp-13-10787-2013

Andrews, D. G., Holton, J. R., & Leovy, C. B. (1987). *Middle atmosphere dynamics* (Vol. 40). San Diego, USA: Academic Press.

Anstey, J. A., Banyard, T. P., Butchart, N., Coy, L., Newman, P. A., Osprey, S., & Wright, C. J. (2021a). Prospect of increased disruption to the qbo in a changing climate. *Geophys. Res. Lett.*. Retrieved from https://www.essoar.org/pdfjs/10.1002/essoar.10503358.3 doi: 10.21203/rs.3.rs-86860/v1

Anstey, J. A., Banyard, T. P., Butchart, N., Coy, L., Newman, P. A., Osprey, S., & Wright, C. J. (2021b). Quasi-biennial oscillation disrupted by abnormal southern hemisphere stratosphere. *Geophys. Res. Lett.*. Retrieved from https://doi.org/10.1002/essoar.10503358.2 doi: 10.1002/essoar.10503358.2

Baldwin, M. P., Gray, L. J., Dunkerton, T. J., Hamilton, K., Haynes, P. H., Randel, W. J., … Takahashi, M. (2001). The quasi-biennial oscillation. *Reviews of Geophysics*, *39*(2), 179–229. doi: 10.1029/1999RG000073

Barton, C. A., & McCormack, J. P. (2017). Origin of the 2016 QBO Disruption and Its Relationship to Extreme El Niño Events. *Geophys. Res. Lett.*. doi: 10.1002/2017GL075576

Butchart, N., & Scaife, A. A. (2001). Removal of chlorofluorocarbons by increased mass exchange between the stratosphere and troposphere in a changing climate. , *410*, 799–802. doi: 10.1038/35071047

Cai, W., Borlace, S., Lengaigne, M., van Rensch, P., Collins, M., Vecchi, G., … Jin, F.-F. (2014). Increasing frequency of extreme El Niño events due to greenhouse warming. *Nat. Clim. Change*, *4*(2), 111-116. doi: 10.1038/nclimate2100

Christiansen, B., Yang, S., & Madsen, M. S. (2016). Do strong warm ENSO events control the phase of the stratospheric QBO? *Geophys. Res. Lett.*, *43*(19), 10,489–10,495. doi: 10.1002/2016GL070751

Coy, L., Newman, P. A., Pawson, S., & Lait, L. R. (2017). Dynamics of the Disrupted 2015/16 Quasi-Biennial Oscillation. *J. Clim.*, *30*(15), 5661-5674. doi: 10.1175/JCLI-D-16-0663.1

DallaSanta, K., Orbe, C., Rind, D., Nazarenko, L., & Jonas, J. (2021). Response of the quasi-biennial oscillation to historical volcanic eruptions. *Geophysical Research Letters*, *48*(20), e2021GL095412. Retrieved from https://agupubs.onlinelibrary.wiley.com/doi/abs/10.1029/2021GL095412 (e2021GL095412 2021GL095412) doi: https://doi.org/10.1029/2021GL095412

Damadeo, R. P., Zawodny, J. M., & Thomason, L. W. (2014). Reevaluation of stratospheric ozone trends from SAGE II data using a simultaneous temporal and spatial analysis. *Atmos. Chem. Phys.*, *14*(24), 13455–13470. doi: 10.5194/acp-14-13455-2014

Dessler, A. E., Schoeberl, M. R., Wang, T., Davis, S. M., & Rosenlof, K. H. (2013). Stratospheric water vapor feedback. *Proceed. Nat. Acad. Sci.*, *110 45*, 18087-91.

Diallo, M., Ern, M., & Ploeger, F. (2021). The advective brewer–dobson circulation in the era5 reanalysis: climatology, variability, and trends. *Atmospheric Chemistry and Physics*, *21*(10), 7515–7544. Retrieved from https://acp.copernicus.org/articles/21/7515/2021/ doi: 10.5194/acp-21-7515-2021

Diallo, M., Konopka, P., Santee, M. L., Müller, R., Tao, M., Walker, K. A., … Ploeger, F. (2019). Structural changes in the shallow and transition branch of the brewer–dobson circulation induced by el niño. *Atmospheric Chemistry and Physics*, *19*(1), 425–446. Retrieved from https://www.atmos-chem-phys.net/19/425/2019/ doi: 10.5194/acp-19-425-2019

Diallo, M., Ploeger, F., Konopka, P., Birner, T., Müller, R., Riese, M., … Jegou, F. (2017). Significant contributions of volcanic aerosols to decadal changes in the stratospheric circulation. *Geophysical Research Letters*, *44*(20), 10,780-10,791. Retrieved from https://agupubs.onlinelibrary.wiley.com/doi/abs/10.1002/2017GL074662 doi: 10.1002/2017GL074662

Diallo, M., Riese, M., Birner, T., Konopka, P., Müller, R., Hegglin, M. I., … Ploeger, F. (2018). Response of stratospheric water vapor and ozone to the unusual timing of el niño and the qbo disruption in 2015–2016. *Atmo-*

*spheric Chemistry and Physics*, *18*(17), 13055–13073. Retrieved from https://www.atmos-chem-phys.net/18/13055/2018/ doi: 10.5194/acp-18-13055-2018

Dunkerton, T. J. (1980). A Lagrangian mean theory of wave, mean-Flow interaction with applications to nonacceleration and its breakdown. *Rev. of Geophys.*, *18*(2), 387–400. doi: 10.1029/RG018i002p00387

Dunkerton, T. J. (2016). The quasi-biennial oscillation of 2015–2016: Hiccup or death spiral? *Geophys. Res. Lett.*, *43*(19), 10,547–10,552. doi: 10.1002/2016GL070921

Ern, M., Diallo, M., Preusse, P., Mlynczak, M. G., Schwartz, M. J., Wu, Q., & Riese, M. (2021). The semiannual oscillation (sao) in the tropical middle atmosphere and its gravity wave driving in reanalyses and satellite observations. *Atmos. Chem. Phys.*, *21*(18), 13763–13795. Retrieved from https://acp.copernicus.org/articles/21/13763/2021/ doi: 10.5194/acp-21-13763-2021

Ern, M., Ploeger, F., Preusse, P., Gille, J. C., Gray, L. J., Kalisch, S., … Riese, M. (2014). Interaction of gravity waves with the QBO: A satellite perspective. *J. Geophys. Res.: Atmospheres*, *119*(5), 2329–2355. doi: 10.1002/2013JD020731

Forster, P. M., & Shine, K. P. (1999). Stratospheric water vapour changes as a possible contributor to observed stratospheric cooling. *Geophys. Res. Lett.*, *26*(21), 3309–3312. doi: 10.1029/1999GL010487

Forster, P. M., & Shine, K. P. (2002). Assessing the climate impact of trends in stratospheric water vapor. *Geophys. Res. Lett.*, *29*(6). doi: 10.1029/2001GL013909

Friston, K., Ashburner, J., Kiebel, S. J., Nichols, T. E., & Penny, W. D. (Eds.). (2007). *Statistical parametric mapping: The analysis of functional brain images.* Academic Press. Retrieved from http://store.elsevier.com/product.jsp?isbn=9780123725608

Fueglistaler, S., Dessler, A. E., Dunkerton, T. J., Folkins, I., Fu, Q., & Mote, P. W. (2009, February). Tropical tropopause layer. *Rev. Geophys.*, *47*, G1004+. doi: 10.1029/2008RG000267

Garfinkel, C. I., Hurwitz, M. M., Oman, L. D., & Waugh, D. W. (2013). Contrasting Effects of Central Pacific and Eastern Pacific El Niño on stratospheric water vapor. *Geophys. Res. Lett.*, *40*(15), 4115–4120. doi: 10.1002/grl.50677

Geller, M. A., Zhou, X., & Zhang, M. (2002). Simulations of the Interannual Variability of Stratospheric Water Vapor. *J. Atmos. Sci.*, *59*(6), 1076-1085. doi: 10.1175/1520-0469(2002)059$⟨$1076:SOTIVO$⟩$2.0.CO;2

Gettelman, A., Hoor, P., Pan, L. L., Randel, W. J., Hegglin, M. I., & Birner, T. (2011). The extratropical upper troposphere and lower stratosphere. *Rev. Geophys.*, *49*, RG3003. doi: 10.1029/2011RG000355

Grimshaw, R. (1984). Wave Action and Wave–Mean Flow Interaction, with Application to Stratified Shear Flows. *Annual Rev. of Fluid Mech.*, *16*(1), 11-44. doi: 10.1146/annurev.fl.16.010184.000303

Hartmann, D. L., Holton, J. R., & Fu, Q. (2001). The heat balance of the tropical tropopause, cirrus, and stratospheric dehydration. *Geophys. Res. Lett.*, *28*(10), 1969–1972. doi: 10.1029/2000GL012833

Haynes, P. H., McIntyre, M. E., Shepherd, T. G., Marks, C. J., & Shine, K. P. (1991). On the "downward control" of extratropical diabatic circulations by eddy-induced mean zonal forces. *J. Atmos. Sci.*, *48*(4), 651-678. doi: 10.1175/1520-0469(1991)048$⟨$0651:OTCOED$⟩$2.0.CO;2

Haynes, P. H., & Shuckburgh, E. (2000). Effective diffusivity as a diagnostic of atmospheric transport 2. Troposphere and lower stratosphere. *J. Geophys. Res.*, *105*(D18), 22795–22810. doi: 10.1029/2000JD900092

Hegglin, M. I., Tegtmeier, S., Anderson, J., Bourassa, A. E., Brohede, S., Degenstein, D., … Weigel, K. (2021). Overview and update of the sparc data initiative: comparison of stratospheric composition measurements from satellite limb sounders. *Earth Syst. Sci. Data*, *13*(5), 1855–1903. Retrieved from `https://essd.copernicus.org/articles/13/1855/2021/` doi: 10.5194/essd-13-1855-2021

Hegglin, M. I., Tegtmeier, S., Anderson, J., Froidevaux, L., Fuller, R., Funke, B., … Weigel, K. (2013). Sparc data initiative: Comparison of water vapor climatologies from international satellite limb sounders. *J. Geophys. Res.: Atmospheres*, *118*(20), 11,824-11,846. doi: 10.1002/jgrd.50752

Hersbach, H., Bell, B., Berrisford, P., Hirahara, S., Horányi, A., Muñoz-Sabater, J., … Thépaut, J.-N. (2020). The era5 global reanalysis. *Q. J. R. Meteorol. Soc.*, *n/a*(n/a). Retrieved from `https://rmets.onlinelibrary.wiley.com/doi/abs/10.1002/qj.3803` doi: 10.1002/qj.3803

Hitchcock, P., Haynes, P. H., Randel, W. J., & Birner, T. (2018). The Emergence of Shallow Easterly Jets within QBO Westerlies. *J. Atmos. Sci.*, *75*(1), 21-40. doi: 10.1175/JAS-D-17-0108.1

Holton, J. R. (1979). Equatorial Wave-Mean Flow Interaction: A Numerical Study of the Role of Latitudinal Shear. *J. Atmos. Sci.*, *36*(6), 1030-1040. doi: 10.1175/1520-0469(1979)036$⟨$1030:EWMFIA$⟩$2.0.CO;2

Holton, J. R., & Gettelman, A. (2001). Horizontal transport and the dehydration of the stratosphere. *Geophys. Res. Lett.*, *28*(14), 2799–2802. doi: 10.1029/2001GL013148

Hu, D., Tian, W., Guan, Z., Guo, Y., & Dhomse, S. (2016). Longitudinal Asymmetric Trends of Tropical Cold-Point Tropopause Temperature and Their Link to Strengthened Walker Circulation. *J. Clim.*, *29*(21), 7755-7771. doi: 10.1175/JCLI-D-15-0851.1

Ihara, C., Kushnir, Y., & Cane, M. A. (2008). Warming trend of the indian ocean sst and indian ocean dipole from 1880 to 2004. *J. of Clim.*, *21*(10), 2035 - 2046. Retrieved from `https://journals.ametsoc.org/view/journals/clim/21/10/2007jcli1945.1.xml` doi: 10.1175/2007JCLI1945.1

Jensen, E. J., Toon, O. B., Pfister, L., & Selkirk, H. B. (1996). Dehydration of the upper troposphere and lower stratosphere by subvisible cirrus clouds near the tropical tropopause. *Geophys. Res. Lett.*, *23*(8), 825–828. doi: 10.1029/96GL00722

Jia, J. Y., Preusse, P., Ern, M., Chun, H.-Y., Gille, J. C., Eckermann, S. D., & Riese, M. (2014). Sea surface temperature as a proxy for convective gravity wave excitation: a study based on global gravity wave observations in the middle atmosphere. *Annales Geophysicae*, *32*(11), 1373–1394. Retrieved from `https://angeo.copernicus.org/articles/32/1373/2014/` doi: 10.5194/angeo-32-1373-2014

Kalnay, E., Kanamitsu, M., Kistler, R., Collins, W., Deaven, D., Gandin, L., … Joseph, D. (1996). The ncep/ncar 40-year reanalysis project. *Bulletin of the American Meteorological Society*, *77*(3), 437 - 472. Retrieved from `https://journals.ametsoc.org/view/journals/bams/77/3/1520-0477_1996_077_0437_tnyrp_2_0_co_2.xml` doi: 10.1175/1520-0477(1996)077⟨0437:TNYRP⟩2.0.CO;2

Kang, M.-J., & Chun, H.-Y. (2021). Contributions of equatorial planetary waves and small-scale convective gravity waves to the 2019/20 qbo disruption. *Atmos. Chem. Phys.*, *2021*, 1–33. Retrieved from `https://acp.copernicus.org/preprints/acp-2021-85/` doi: 10.5194/acp-2021-85

Kang, M.-J., Chun, H.-Y., & Garcia, R. R. (2020). Role of equatorial waves and convective gravity waves in the 2015/16 quasi-biennial oscillation disruption. *Atmos. Chem. Phys.*, *20*(23), 14669–14693. Retrieved from `https://acp.copernicus.org/articles/20/14669/2020/` doi: 10.5194/acp-20-14669-2020

Kawatani, Y., & Hamilton, K. (2013). Weakened stratospheric quasibiennial oscillation driven by increased tropical mean upwelling. *Nature*, *497*, 478–481. doi: doi:

10.1038/nature12140

Kawatani, Y., Hamilton, K., & Watanabe, S. (2011). The Quasi-Biennial Oscillation in a Double CO2 Climate. *J. Atmos. Sci.*, *68*(2), 265-283. doi: 10.1175/2010JAS3623.1

Khaykin, S., Legras, B., & Bucci, S. e. a. (2020). The 2019/20 australian wildfires generated a persistent smoke-charged vortex rising up to 35km altitude. *Commun. Earth Environ.*, *1*(22). doi: 10.1038/s43247-020-00022-5

Kim, J., & Alexander, M. J. (2015). Direct impacts of waves on tropical cold point tropopause temperature. *Geophys. Res. Lett.*, *42*(5), 1584-1592. doi: https://doi.org/10.1002/2014GL062737

Kim, J., & Son, S.-W. (2012). Tropical Cold-Point Tropopause: Climatology, Seasonal Cycle, and Intraseasonal Variability Derived from COSMIC GPS Radio Occultation Measurements. *Journal of Climate*, *25*(15), 5343-5360. doi: 10.1175/JCLI-D-11-00554.1

Kroll, C. A., Dacie, S., Azoulay, A., Schmidt, H., & Timmreck, C. (2020). The impact of volcanic eruptions of different magnitude on stratospheric water vapour in the tropics. *Atmos. Chem. Phys.*, *2020*, 1–45. Retrieved from `https://acp.copernicus.org/preprints/acp-2020-1191/` doi: 10.5194/acp-2020-1191

Liess, S., & Geller, M. A. (2012). On the relationship between QBO and distribution of tropical deep convection. *J. Geophys. Res.: Atmospheres*, *117*(D3). doi: 10.1029/2011JD016317

Livesey, N. J., Read, W. G., Wagner, P. A., Froidevaux, L., Lambert, A., Manney, G. L., ... Martinez, E. (2017). Aura Microwave Limb Sounder (MLS) Version 4.2x Level 2 data quality and description document. *Tech. Rep. JPL D-33509 Rev. C*, 1–169. doi: 10.5194/acp-15-9945-2015

Newman, P. A., Coy, L., Pawson, S., & Lait, L. R. (2016). The anomalous change in the QBO in 2015–2016. *Geophys. Res. Lett.*, *43*(16), 8791–8797. doi: 10.1002/2016GL070373

Newman, P. A., & Nash, E. R. (2000). Quantifying the wave driving of the stratosphere. *J. Geophys. Res.: Atmospheres*, *105*(D10), 12485–12497. doi: 10.1029/1999JD901191

Niwano, M., Yamazaki, K., & Shiotani, M. (2003, December). Seasonal and qbo variations of ascent rate in the tropical lower stratosphere as inferred from uars haloe trace gas data. *J. Geophys. Res.*, *108*(D24), 4794. (4794) doi: 10.1029/2003JD003871

Nowack, P., Abraham, N., Maycock, A., Braesicke, P., Gregory, J., Joshi, M., ... Pyle, J. (2015, January). A large ozone-circulation feedback and its implications for global warming assessments. *Nature Climate Change*, *5*, 41–45. doi: 10.1038/NCLIMATE2451

Osprey, S. M., Butchart, N., Knight, J. R., Scaife, A. A., Hamilton, K., Anstey, J. A., ... Zhang, C. (2016, September 08). An unexpected disruption of the atmospheric quasi-biennial oscillation. *Science*. doi: 10.1126/science.aah4156

Plumb, R. A. (2002). Stratospheric transport. *J. Meteor. Soc. Japan*, *80*, 793-809.

Randel, W. J., Park, M., Wu, F., & Livesey, N. (2007). A Large Annual Cycle in Ozone above the Tropical Tropopause Linked to the Brewer Dobson Circulation. *J. Atmos. Sci.*, *64*(12), 4479–4488. doi: 10.1175/2007JAS2409.1

Randel, W. J., & Thompson, A. M. (2011). Interannual variability and trends in tropical ozone derived from sage ii satellite data and shadoz ozonesondes. *Journal of Geophysical Research: Atmospheres*, *116*(D7). Retrieved from `https://agupubs.onlinelibrary.wiley.com/doi/abs/10.1029/2010JD015195` doi: https://doi.org/10.1029/2010JD015195

Riese, M., Ploeger, F., Rap, A., Vogel, B., Konopka, P., Dameris, M., & Forster, P. (2012). Impact of uncertainties in atmospheric mixing on simulated utls composition and related radiative effects. *J. Geophys. Res.*, *117*. doi:

10.1029/2012JD017751
Rosenlof, K., & Holton, J. (1993). Estimates of the stratospheric residual circulation using the downward control principle. *J. Geophys. Res.*, *98*, 10,465-10,479.
Saji, N., Goswami, B., Vinayachandran, P., & Yamagata, T. (1999, September). A dipole mode in the tropical indian ocean. *Nature*, *401*(6751), 360—363. Retrieved from https://doi.org/10.1038/43854 doi: 10.1038/43854
Santee, M. L., Manney, G. L., Livesey, N. J., Schwartz, M. J., Neu, J. L., & Read, W. G. (2017). A comprehensive overview of the climatological composition of the Asian summer monsoon anticyclone based on 10 years of Aura Microwave Limb Sounder measurements. *J. Geophys. Res.: Atmospheres*, *122*(10), 5491–5514. doi: 10.1002/2016JD026408
Saravanan, R. (1990). A Multiwave Model of the Quasi-biennial Oscillation. *J. Atmos. Sci.*, *47*(21), 2465-2474. doi: 10.1175/1520-0469(1990)047$⟨$2465:AMMOTQ$⟩$2.0.CO;2
Schirber, S. (2015). Influence of enso on the qbo: Results from an ensemble of idealized simulations. *J. Geophys. Res.: Atmospheres*, *120*(3), 1109–1122. doi: 10.1002/2014JD022460
Schoeberl, M. R., & Dessler, A. E. (2011, August). Dehydration of the stratosphere. *Atmos. Chem. Phys.*, *11*, 8433-8446. doi: 10.5194/acp-11-8433-2011
Shepherd, T. G. (2007). Transport in the middle atmosphere. *J. Meteorol. Soc. of Japan. Ser. II*, *85B*, 165-191. doi: 10.2151/jmsj.85B.165
Shepherd, T. G., & McLandress, C. (2011). A robust mechanism for strengthening of the brewer–dobson circulation in response to climate change: Critical-layer control of subtropical wave breaking. *J. Atmos. Sci.*, *68*(4), 784-797. Retrieved from https://doi.org/10.1175/2010JAS3608.1 doi: 10.1175/2010JAS3608.1
Smith, J. W., Haynes, P. H., Maycock, A. C., Butchart, N., & Bushell, A. C. (2021). Sensitivity of stratospheric water vapour to variability in tropical tropopause temperatures and large-scale transport. *Atmospheric Chemistry and Physics*, *21*(4), 2469–2489. Retrieved from https://acp.copernicus.org/articles/21/2469/2021/ doi: 10.5194/acp-21-2469-2021
Solomon, S., Rosenlof, K. H., Portmann, R. W., Daniel, S. M., J. S. Davis, Sanford, T., & Plattner, G.-K. (2010). Contributions of Stratospheric Water Vapor to Decadal Changes in the Rate of Global Warming. *Science*, *327*(5970), 1219–1223. doi: 10.1126/science.1182488
Son, S.-W., Lim, Y., Yoo, C., Hendon, H. H., & Kim, J. (2017). Stratospheric control of the madden–julian oscillation. *Journal of Climate*, *30*(6), 1909 - 1922. Retrieved from https://journals.ametsoc.org/view/journals/clim/30/6/jcli-d-16-0620.1.xml doi: 10.1175/JCLI-D-16-0620.1
Taguchi, M. (2010). Observed connection of the stratospheric quasi-biennial oscillation with El Niño–Southern Oscillation in radiosonde data. *J. Geophys. Res.: Atmospheres*, *115*(D18). doi: 10.1029/2010JD014325
Tao, M., Konopka, P., Ploeger, F., Yan, X., Wright, J. S., Diallo, M., … Riese, M. (2019). Multitimescale variations in modeled stratospheric water vapor derived from three modern reanalysis products. *Atmos. Chem. Phys.*, *19*(9), 6509–6534. Retrieved from https://acp.copernicus.org/articles/19/6509/2019/ doi: 10.5194/acp-19-6509-2019
Thomason, L. W., Ernest, N., Millán, L., Rieger, L., Bourassa, A., Vernier, J.-P., … Peter, T. (2018). A global space-based stratospheric aerosol climatology: 1979–2016. *Earth Sys. Sci. Data*, *10*(1), 469–492. doi: 10.5194/essd-10-469-2018
Tian, E. W., Su, H., Tian, B., & Jiang, J. H. (2019). Interannual variations of water vapor in the tropical upper troposphere and the lower and middle stratosphere and their connections to enso and qbo. *Atmospheric Chemistry and Physics*, *19*(15), 9913–9926. Retrieved from https://acp.copernicus.org/articles/19/9913/2019/ doi: 10.5194/acp-19-9913-2019

Timmermann, A., Oberhuber, J., Bacher, A., Esch, M., Latif, M., & Roeckner, E. (1999). El Niño, La Nina, and the Southern Oscillation. *Nature*, *398*(6729), 904-905. doi: 10.1038/19505

Tweedy, O. V., Kramarova, N. A., Strahan, S. E., Newman, P. A., Coy, L., Randel, W. J., … Frith, S. M. (2017). Response of trace gases to the disrupted 2015–2016 quasi-biennial oscillation. *Atmos. Chem. Phys.*, *17*(11), 6813–6823. doi: 10.5194/acp-17-6813-2017

von Storch, H., & Zwiers, F. W. (1999). *Statistical analysis in climate research.* Cambridge Unv. Press.

WMO. (2018). *Scientific Assessment of Ozone Depletion: 2018* (Global Ozone Research and Monitoring Project - Report No. 58). Geneva: WMO (World Meteorological Organization).

Wolter, K., & Timlin, M. S. (2011). El Nino/Southern Oscillation behaviour since 1871 as diagnosed in an extended multivariate ENSO index (MEI.ext). *Int. J. Climatol.*, *31*, 1074–1087. doi: 10.1002/joc.2336

Yu, P., Davis, S. M., Toon, O. B., Portmann, R. W., Bardeen, C. G., Barnes, J. E., … Rosenlof, K. H. (2021). Persistent stratospheric warming due to 2019-2020 australian wildfire smoke. *Geophys. Res. Lett.*, *48*(7), e2021GL092609. Retrieved from `https://agupubs.onlinelibrary.wiley.com/doi/abs/10.1029/2021GL092609` (e2021GL092609 2021GL092609) doi: https://doi.org/10.1029/2021GL092609

# Supporting Information for "Stratospheric water vapor and ozone response to different QBO disruption events in 2016 and 2020"

Mohamadou Diallo[1], Felix Ploeger[1,2], Michaela I. Hegglin[3], Manfred Ern[1],

Jens-Uwe Grooß[1], Sergey Khaykin[4] and Martin Riese[1,2]

[1]Institute of Energy and Climate Research, Stratosphere (IEK–7), Forschungszentrum Jülich, 52 425 Jülich, Germany.

[2]Institute for Atmospheric and Environmental Research, University of Wuppertal, Wuppertal, Germany.

[3]Department of Meteorology, University of Reading, Reading, UK.

[4]Laboratoire Atmosphères, Milieux, Observations Spatiales, UMR CNRS 8190, IPSL, Sorbonne Univ./UVSQ, Guyancourt, France.

## Additional Supporting Information

1. Figures S1 to S5

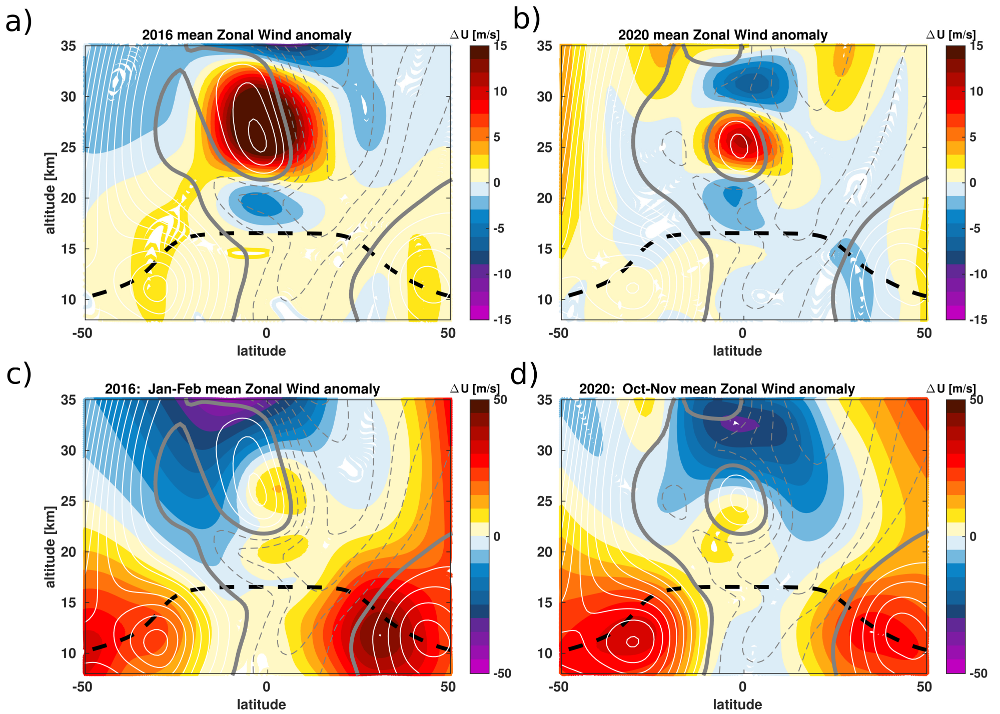


**Figure S1.** zonal mean deseasonalized zonal wind **(a, b)** and the QBO disruption onsets **(c, d)** from the ERA5 reanalysis for the years 2016 **(a, c)** and 2020 **(b, c)** period as a function of latitude and altitude. The black dashed horizontal line indicates the tropopause from ERA5. Monthly mean zonal mean wind component, $u$ ($\mathrm{m\,s^{-1}}$), from ERA5 is overlaid as solid white (westerly) and dashed gray (easterly) lines.

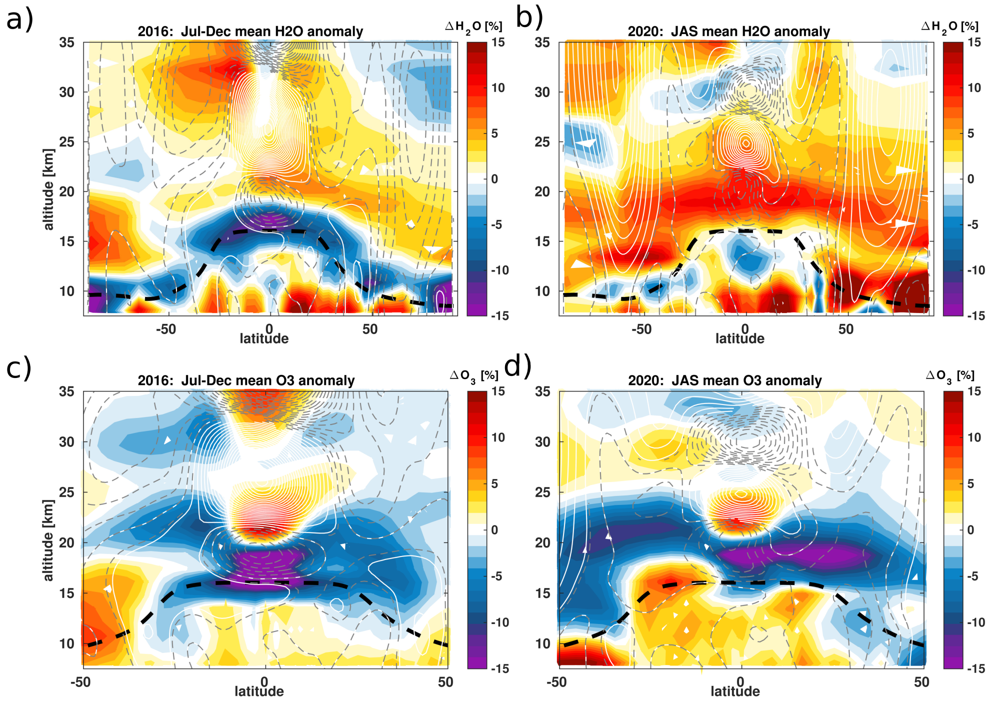


**Figure S2.** zonal mean deseasonalized stratospheric $H_2O$ **(a, b)** and $O_3$ **(c, d)** anomalies from MLS satellite observations for the years 2016 **(a, c)** and 2020 **(b, c)** period in percent change from long-term monthly means as a function of time and altitude. The black dashed horizontal line indicates the tropopause from ERA5. Monthly mean zonal mean wind component, $u$ ($\mathrm{m\,s^{-1}}$), from ERA5 is overlaid as solid white (westerly) and dashed gray (easterly) lines.

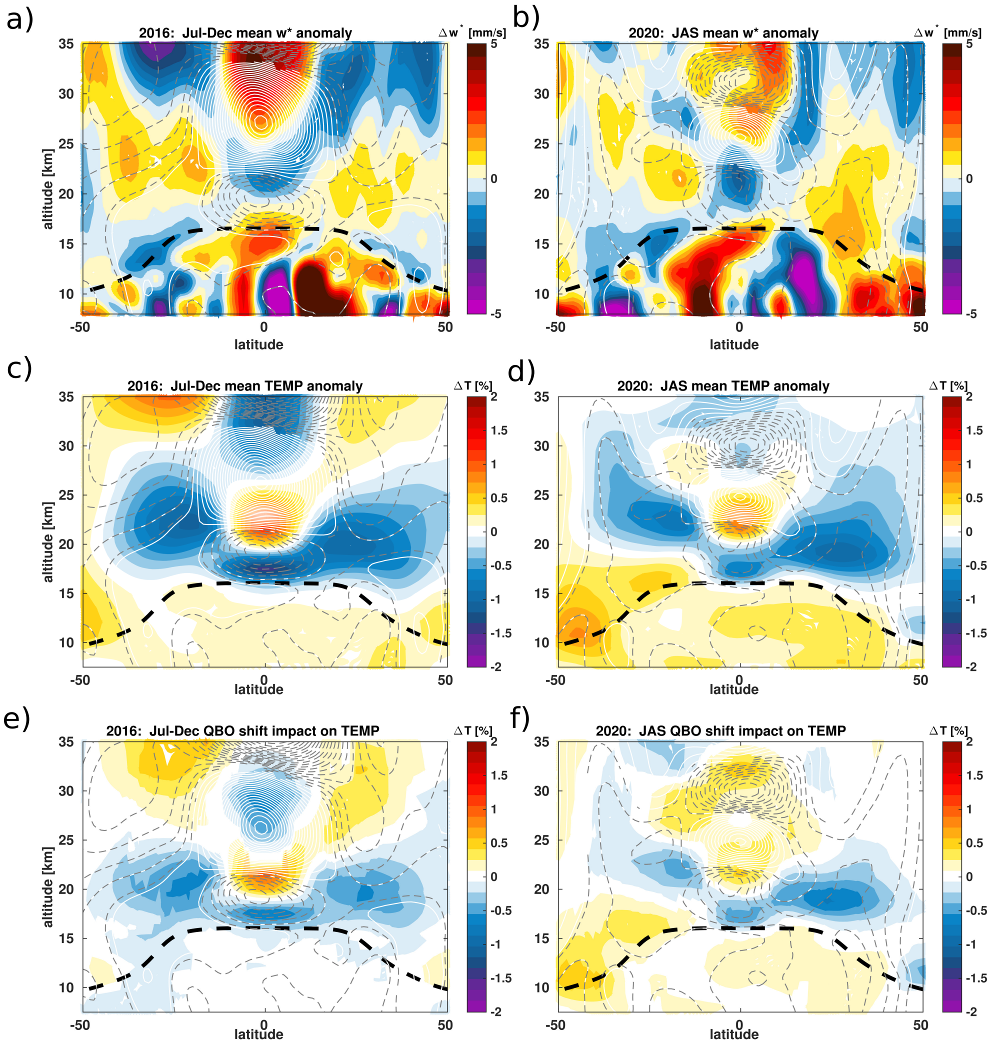


**Figure S3.** zonal mean residual vertical velocity ($\overline{w^*}$) **(a, b)** and temperature anomalies **(c, d)** together with the impact of QBO disruptions on the tropical temperature anomalies **(e, f)** derived from the multiple regression fit for the years 2016 and 2020. The black dashed horizontal line indicates the tropopause from ERA5. Monthly mean zonal mean wind component, $u$ ($\mathrm{m\,s^{-1}}$), from ERA5 is overlaid as solid white (westerly) and dashed gray (easterly) lines.

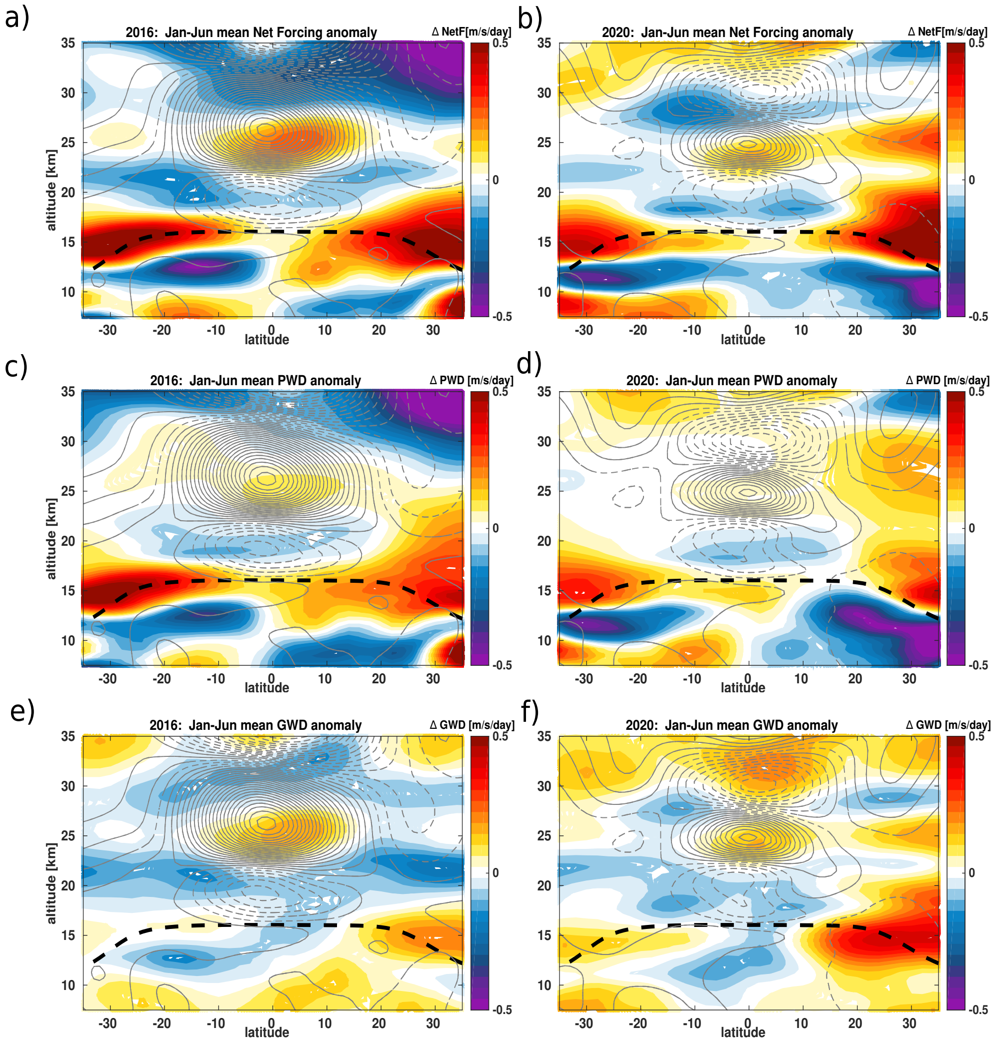


**Figure S4.** zonal mean monthly mean net wave forcing **(a, b)**, planetary wave drag (PWD) **(c, d)** and gravity wave drag (GWD) **(e, f)** anomalies from the ERA5 reanalysis for the years 2016 **(a, c, e)** and 2020 **(b, d, f)** as a function of latitude and altitude. The black dashed horizontal line indicates the tropopause from ERA5. Monthly mean zonal mean wind component, $u$ ($\mathrm{m\,s^{-1}}$), from ERA5 is overlaid as solid gray (westerly) and dashed gray (easterly) lines.

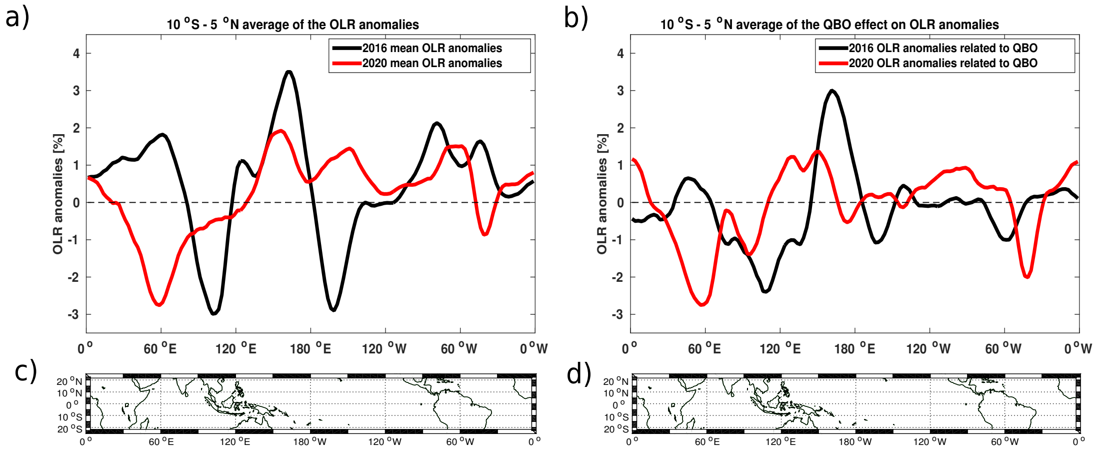


**Figure S5.** Longitudinal variations of the monthly mean Outgoing Longwave Radiation (OLR) anomalies **(a)** averaged between $20^o$ S–$20^o$ S together with the 2016 and 2020 QBO effect **(b)** associated with the convective activity derived from the multiple regression fit. The lowermost panels **(c, d)** shows the QBO index at $50\,hPa$ in red.